

pubs.acs.org/cm Article

Creating a Green-Emitting Phosphor through Selective Rare-Earth Site Preference in NaBaB₉O₁₅:Eu²⁺

Ya Zhuo, Shruti Hariyani, Jiyou Zhong, and Jakoah Brgoch*



Cite This: Chem. Mater. 2021, 33, 3304-3311



Read Online

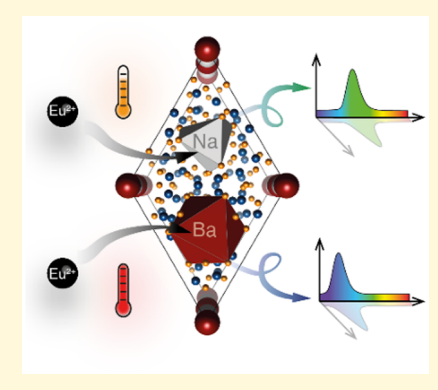
ACCESS

Metrics & More



SI Supporting Information

ABSTRACT: Highly efficient, thermally stable phosphors excited by blue LEDs are crucial for energy-efficient light bulbs and modern display applications. These materials are a central component in these devices, and here one of the first Eu²+-substituted greenemitting borate phosphors is demonstrated. The green emission in NaBaB₉O₁₅:Eu²+ stems from Eu²+ occupying the smaller [NaO₆] polyhedron instead of the larger [BaO₉] polyhedron. This preferential substitution is identified by using quantum mechanical calculations and supported by high-resolution synchrotron X-ray powder diffraction and photoluminescence data. The resulting green emission peak is centered at 515 nm with a quantum yield of >80% ($\lambda_{\rm ex}=430$ nm). This phosphor also exhibits negligible thermal quenching up to 650 K due to the wide bandgap, high connectivity of the rigid NaBaB₉O₁₅ crystal structure, and the depopulation of trap states stemming from the aliovalent rare-earth substitution. Fabricating two blue light pumped LED prototypes with NaBaB₉O₁₅:Eu²+ as the green component and a second red-emitting phosphor



demonstrates this novel material's capabilities in both display and warm white lighting formats. Alongside the outstanding optical properties, the accessible synthetic conditions and cost-effective starting materials suggest the remarkable potential of $NaBaB_9O_{15}$: Eu^{2+} in next-generation LED-based lighting or display systems.

■ INTRODUCTION

Phosphor-converted white light-emitting diodes (pc-wLED) are the most promising source of next-generation backlighting display technologies and general white lighting. They have high efficiency, long operating life, low energy consumption, and environmentally benign components. These devices operate by converting the nearly monochromatic emission from a LED chip with one or more rare-earth- or transition-metal-substituted inorganic phosphors. Recent research by groups around the world has yielded a plethora of new and improved phosphors for these applications. However, even with the successful discovery of many new materials, there remains a significant lack of green phosphors reported in the literature. Considering that the human eye is most sensitive to the green spectral region, there is a need to identify new efficient greenemitting phosphors.

Only a few green phosphors fulfill the stringent requirements for application, including an appropriate peak position, a high efficiency, and excellent thermal stability. β -SiAlON:Eu²⁺ is the narrowest commercial green phosphor available today, but its emission coordinates limit the maximum accessible color gamut. The synthesis of β -SiAlON:Eu²⁺ also requires high-pressure and high-temperature conditions, increasing the material's cost. (Ba,Sr)₂SiO₄:Eu²⁺ and SrGa₂S₄:Eu²⁺ are easier to prepare, requiring only high-temperature solid-state reaction under mild reducing conditions. Nevertheless, the broad emission band of the former and the poor thermal and chemical stability of the latter remain a challenge. (13,14)

green-emitting phosphor is Ca₈Mg(SiO₄)₄Cl₂:Eu²⁺. This compound shows an intense emission with the peak centered at 505 nm. 15 However, this phase shows persistent luminescence, which is not ideal for general lighting applications. Recently, RbLi(Li₃SiO₄)₂:Eu²⁺ and Ba_{2-x}LiAlS₄:Eu²⁺ were also reported to be highly efficient phosphors with a narrow emission band, but their chemical stability must be enhanced for industrial applications. 16,17 Most recently, quantum dot (QD) emitters have also been demonstrated as a potential alternative solution with significant advantages, particularly for display lighting. Research continues to address their chemical and thermal stability and their toxic chemical compositions. 18,19 Clearly, additional applicationready green-emitting phosphors are required, which has propelled researchers to establish new design strategies and investigate unconventional crystal chemistries.

There has been a refocus on borate phosphors because of their easy synthesis process, diverse crystal structures and compositions, and excellent chemical and physical stability. However, at present, the luminescence of nearly all borate

Received: February 7, 2021 Revised: April 22, 2021 Published: April 30, 2021





phosphors, regardless of substitution with Eu²⁺ or Ce³⁺, produces a blue emission (420-450 nm) after excitation with a UV source.²⁰ There are virtually no other examples of borates that have electronic transitions outside of this region. The only exception was the report of NaBaBO3:Ce3+, which was suggested to produce a green emission centered at 505 nm. 21 Interestingly, this phase is the only member in the $MNBO_3$ (M = Li, Na; N = Ca, Sr, Ba) family that emits a color other than blue. Subsequent work on NaBaBO₃:Ce³⁺ failed to reproduce the green emission and instead yielded a blue emission.²² Using quantum mechanical calculations, we attributed this discrepancy in emission wavelengths to the rare-earth ion substituting on different crystallographic sites. The results indicate that when Ce³⁺ replaces Ba²⁺ in the crystal structure, a blue emission is expected, whereas a green emission is expected when Ce³⁺ occupies the Na⁺ position. The change in emission colors stems from the smaller polyhedral volume of the [NaO₆] compared to the [BaO₉], causing stronger crystal field splitting of Ce3+ 5d orbitals. Although the successive work could not achieve the preferential substitution necessary to switch the emission color, these results propose that non-blue-emitting borate phosphors may be possible provided the rare-earth ion can be selectively substituted for Na⁺. The research presented here aims to prove this connection by selectively placing the rareearth ion on the (energetically) nonpreferred Na+ site in inorganic borate phosphors.

Our group recently reported a different borate phosphor within the Na₂O-BaO-B₂O₃ system with the general formula Na(Ba_{0.97}Eu_{0.03})B₉O₁₅.²³ The crystal structure adopts the noncentrosymmetric trigonal space group R3c (space group no. 161).²⁴ As illustrated in Figure 1a, the structure contains an

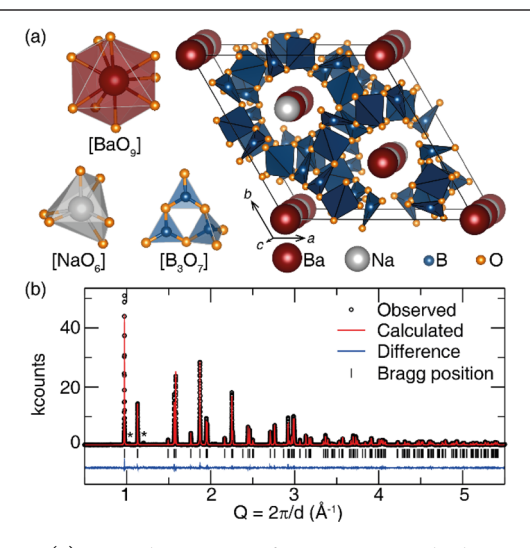


Figure 1. (a) Crystal structure of NaBaB₉O₁₅ with the associated [BaO₉], [NaO₆], and [B₃O₇] polyhedral subunits highlighted. (b) Rietveld refinement of (Na_{0.97}Eu_{0.03})BaB₉O₁₅ synchrotron X-ray powder diffraction data. Asterisks mark the minor BaB₈O₁₃ impurity.

unusual three-dimensional framework of $[B_3O_7]^{5-}$ subunits composed of two $[BO_3]^{3-}$ trigonal planar units and one $[BO_4]^{5-}$ tetrahedron linked through their vertices. The arrangement of the $[B_3O_7]^{5-}$ units generates large tunnels along the [001] direction that are occupied by Ba^{2+} and Na^+ in an alternating fashion. The Ba^{2+} ions are coordinated in a ninevertex distorted tricapped trigonal prism. Na^+ sits in a smaller,

highly distorted trigonal antiprism formed by six oxygen anions. The original synthesis of this phosphor uses a multistep solid-state reaction at >750 °C with metal oxides and carbonates as starting materials. Under these conditions, Eu²⁺ replaces Ba²⁺ to generate a highly efficient, narrow blue emission ($\lambda_{\rm em}=416$ nm) by using UV excitation ($\lambda_{\rm ex}=315$ nm).²³

In this work, we employed DFT calculations to show that Eu²⁺ substitution on the Na⁺ antisite and the predictable isovalent Ba²⁺ site exhibit similar formation energies. The rareearth substitution on both crystallographic sites is thus an energetically competitive process. The green version of NaBaB₉O₁₅:Eu²⁺ was then achieved by modifying the synthetic route to drive the substitution of Eu²⁺ onto the Na⁺-centered polyhedral site. Owing to the smaller volume of the [NaO₆] polyhedron compared to the larger [BaO₉] unit, (Na_{0.97}Eu_{0.03})-BaB₀O₁₅ emits at the longer wavelength, as expected, following the enhanced crystal field splitting of the Eu²⁺ 5d orbitals. This phosphor not only shows a green emission under blue excitation, but it exhibits a high photoluminescence quantum yield (Φ) and excellent thermal stability. The fabricated device prototypes using (Na_{0.97}Eu_{0.03})BaB₉O₁₅ suggest this bright green phosphor is applicable for general white lighting or display applications. More importantly, the concept of controlling preferential substitution will provide new opportunities for the discovery of luminescent materials.

■ EXPERIMENTAL SECTION

Computational Details. All density functional calculations were conducted by using the Vienna ab initio simulation package (VASP) with projector-augment-wave (PAW) pseudopotentials. ^{25,26} The host crystal structure was relaxed by using generalized gradient approximation PBE functionals. ²⁷ The PBE+U method with a U = 7.62 was employed to relax the structures of Eu²⁺-doped phosphors. ²⁸ The electronic convergence criterion and ionic convergence criterion were set to be 2×10^{-6} eV and 0.01 eV/Å, respectively. A cutoff energy of 500 eV was used for the basis set of the plane waves, and a 5 × 5 × 3 Γ-centered Monkhorst–Pack k-point grid was used to sample the first Brillouin zone. Formation energies of the Eu²⁺-doped structure were estimated by using $E_f = E_{tot}^D - E_{tot}^H$, where E_{tot}^D and E_{tot}^H are the total energies of the doped structure and the undoped host, respectively.

Sample Preparation and Characterization. (Na_{0.97}Eu_{0.03})- BaB_9O_{15} and $Na(Ba_{0.97}Eu_{0.03})B_9O_{15}$ were prepared via solid-state reactions starting from NaHCO₃ (EM Science, 99.7%), BaCO₃ (Johnson Matthey, 98%), H₃BO₃ (Sigma-Aldrich, 99.999%), and Eu₂O₃ (Materion Advanced Chemicals, 99.9%). The starting materials were loaded in the requisite stoichiometric ratios, thoroughly ground by using an agate mortar and pestle. The freshly grounded mixture for Na(Ba_{0.97}Eu_{0.03})B₉O₁₅ subsequently sintered at 600 °C for 2 h in the air to decompose the reagents and initiate the reaction. The samples were then ground and heated at 780 °C for 30 h by using a fused silica tube furnace under a weak reducing atmosphere (5% $H_2/95\%$ N_2) with heating and cooling ramps of 3 °C min^{-1} . The mixture to make $(Na_{0.97}Eu_{0.03})BaB_9O_{15}$ was stored in the air for 2 weeks and then heated at 600 °C for 2 h in the air followed by 725 $^{\circ}\text{C}$ for 30 h under the reducing atmosphere with one intermediate grinding in between the two heating steps. All products were ground into a fine powder by using an agate mortar and pestle before conducting characterizations.

Synchrotron X-ray powder diffraction data were collected at 295 K with a calibrated wavelength of 0.412824 Å (beamline 11-BM, Advanced Photon Source, Argonne National Laboratory). The crystal lattice parameters were obtained from refinements based on the Rietveld method by using the GSAS package with a shifted Chebyshev function employed to describe the background and a pseudo-Voigt function for determining peak shape. 30,31 All other X-

ray patterns were collected with a Panalytical X'Pert Pro powder X-ray diffractometer equipped with Cu K α radiation (λ = 1.54183 Å). The scanning electron microscopy (SEM) images and energy-dispersive X-ray spectroscopy (EDS) elemental mappings were collected on a Hitachi-S4800 (Japan).

Optical Measurement. The sample was mixed into silicone resin (GE Silicones, RTV615) and deposited on a quartz substrate (Chemglass). Photoluminescent spectra were recorded on a Horiba Fluoromax-4 fluorescence spectrophotometer with a 75 W xenon arc lamp with temperature controlled by a Janis liquid nitrogen cryostat (VPF-100). The luminescence lifetime decay measurements were collected by using a Horiba DeltaFlex Lifetime System equipped with a NanoLED N-390 nm LED ($\lambda_{\rm ex}$ = 392 nm) and a 450 nm long-pass filter. A total measurement length of 13 μ s was employed with a repetition rate of 50 kHz and a delay of 10 ns. The photoluminescence quantum yield (PLQY) and external quantum efficiency (EQE) were determined by placing the sample inside a Spectraloncoated integrating sphere (150 mm diameter, Labsphere) and exciting with n-UV through blue light of different wavelengths.³² The thermoluminescence (TL) curves were collected by a thermoluminescence meter (SL08-L, Guangzhou-Radiation Science and Technology Co. Ltd.) with the heating rate of 1 K/s after being excited (λ_{ex} = 254 nm) for 10 min. The fabrication of the pc-wLED devices involved the addition of commercial red-emitting K₂SiF₆:Mn⁴⁺ (Stanford Advanced Materials), laboratory-made red-emitting Sr₂Si₅N₈:Eu²⁺, and the green-emitting (Na_{0.97}Eu_{0.03})BaB₉O₁₅ phosphor described here in the silicone resin. The corresponding mixture was then coated on a λ_{ex} = 450 nm blue-emitting LED chip (Thorlabs, LED450E). The electroluminescence spectrum, color rendering index (CRI), and correlated color temperature (CCT) of the pc-LED devices were measured under a forward bias of 20 mA by using an AvaFast fiber-optic VIS/NIR spectrometer coupled to a 50 mm integrating sphere.

■ RESULTS AND DISCUSSION

The substitution of Eu²+ for Ba²+ was widely expected based on ionic radii of the elements present in NaBaB₉O₁₅. Eu²+ ($r_{9\text{-coord}}$ = 1.30 Å) has a slightly smaller radius than Ba²+ ($r_{9\text{-coord}}$ = 1.47 Å),³³ which makes it likely for the substitution to occur. Indeed, this is not only observed in Na(Ba_{0.97}Eu_{0.03})B₉O₁₅ but also many other Ba²+ containing phosphors like BaMgA-l₁₀O₁₇:Eu²+ and BaAl₂Si₂O₈:Eu²+ ³·4,³⁵ However, recognizing that the ionic radius of 6-coordinate Eu²+ ($r_{6\text{-coord}}$ = 1.17 Å) is only ≈15% larger than Na⁺ ($r_{6\text{-coord}}$ = 1.02 Å), which is within limits of the Hume–Rothery rules for substitution, suggests it may also be possible for the rare-earth ion to replace the alkali metal instead. Given the presence of both Ba²+ sites and Na⁺ sites in this crystal structure, NaBaB₉O₁₅:Eu²+ provides an additional platform to investigate the relationship between substitution site-preference and the ensuing optical properties in borate phosphors.

The effect of the substitutional site preference on the Eu²⁺ optical properties can first be empirically estimated by following eq 1³⁷

$$E (cm^{-1}) = Q \left[1 - \left(\frac{V}{4} \right)^{1/V} 10^{-nE_a r/80} \right]$$
 (1)

where Q is the position in energy for the lower d-band edge for Eu^{2+} free ion, which is 34000 cm⁻¹, V is the valency of rare-earth ion, n is the number of anions in the immediate shell around Eu^{2+} , $E_{\rm a}$ is the electron affinity of the anions, and r is the radius of the host cation replaced by Eu^{2+} . On the basis of the specific coordination numbers from the refined crystal structure and the corresponding V, $E_{\rm a}$, and r values, the center of the emission peak is estimated to be 24720 cm⁻¹ or 404 nm

for Na(Ba $_{0.97}$ Eu $_{0.03}$)B $_{9}O_{15}$ (NBBO:Eu $_{Ba}$) and 18522 cm $^{-1}$ or 540 nm for (Na $_{0.97}$ Eu $_{0.03}$)BaB $_{9}O_{15}$ (NBBO:Eu $_{Na}$). The difference in optical properties arises from Eu $^{2+}$ occupying the smaller polyhedral volume of the [NaO $_{6}$] site compared to the larger [BaO $_{9}$] unit, which enhances crystal field splitting of the Eu $^{2+}$ 5d orbitals. Therefore, it is expected that if Eu $^{2+}$ can substitute for Na $^{+}$ in NaBaB $_{9}O_{15}$, it may yield an elusive greenemitting borate.

DFT total calculations provide definitive evidence that NaBaB₉O₁₅ may indeed be an ideal system for achieving a new green-emitting borate phosphor through selective site substitution. The Vienna ab initio simulation package was used to determine the formation energy for Eu²⁺ to substitute on each crystallographically independent substitution site. For these calculations, NBBO:EuBa requires only one model due to the single crystallographic site of Ba and the isoelectronic substitution of the divalent ions. In contrast, the NBBO: Eu_{Na} structure requires the formation of defects due to aliovalent substitution. Here, the defects are treated as neutral and include $E{u_{Na}}^{\bullet}$ + ${V_{Na}}^{\prime}$ ($E{u^{2+}}$ entering the Na^{+} site and a vacancy on the Na⁺ site) and Eu_{Na} + Na_{Ba} (Eu²⁺ entering the Na⁺ site and additional Na⁺ entering the Ba²⁺ site). Calculating the formation energies for NBBO:Eu_{Ba} reveals that it takes 3.8 meV/atom to substitute Eu²⁺ on the Ba²⁺ crystallographic position. Intriguingly, Eu²⁺ substituting on the Na⁺ crystallographic sites, modeled by $\mathrm{Eu_{Na}}^{\bullet} + \mathrm{V_{Na}}'$ and $\mathrm{Eu_{Na}}^{\bullet} + \mathrm{Na_{Ba}}'$, shows that it takes only 6.2 meV/atom and 8.3 eV/atom, respectively. Considering NBBO:Eu_{Na} (Eu_{Na}• + Na_{Ba}') is less thermodynamically favorable than NBBO:Eu_{Ba} by only 2.4 meV/atom, there is no strong site preference, and rare-earth substitution should be considered an energetically competitive process. In contrast, calculating the comparable NaBaBO₃ phase shows that it takes 53 meV/atom more energy to substitute Eu²⁺ on the Na⁺ positions compared to Eu²⁺ on the Ba²⁺ position, and it takes 37 meV/atom more energy to substitute Ce³⁺ on the Na⁺ positions compared to Ce³⁺ on the Ba²⁺ position. Obviously, there is a strong preference for rareearth substitution on the Ba2+ site in NaBaBO3, making it problematic to stabilize the rare-earth substitution on the smaller [NaO₆] polyhedron.

The calculations indicate that it may be energetically possible to stabilize Eu²⁺ on the Na⁺ crystallographic position in NaBaB₉O₁₅. At the same time, the empirical model for emission wavelengths suggests the result may be a rare greenemitting borate phosphor. Because the difference in total energy for substitution Eu 2+ on the two sites (Na+ and Ba2+) is only 4.6 meV (or ~54 K), adjusting the synthetic route to lower temperatures may allow the metastable substitution of Eu²⁺ onto the Na⁺-centered polyhedral site. The preparation of the new NBBO:Eu_{Na} phosphor was ultimately achieved by reacting the starting materials at lower temperatures and including an initial, spontaneous prereaction step. This "aging" process involved grinding stoichiometric amounts of the starting materials and keeping the mixture under atmosphere conditions (21 °C; ~55% room humidity) for 2 weeks. To compare, another set of starting materials was held in a desiccator. Powder X-ray diffraction during the aging process (Figure S1) shows that the mixture kept in air undergoes a spontaneous reaction with the H₃BO₃ and BaCO₃ peaks completely dissolved into the background and ending up with a significant number of low-intensity peaks, whereas the phases stored in the desiccator remain unchanged. The chemical activity of H₃BO₃ is significantly enhanced by absorbing

Table 1. Rietveld Refinement Results Obtained Using Synchrotron X-ray Diffraction Data

formula	$Na(Ba_{0.97}Eu_{0.03})B_9O_{15}$	$NaBaB_9O_{15}^{23}$	$({\rm Na_{0.97}Eu_{0.03}}){\rm BaB_9O_{15}}$
radiation type; λ (Å)	synchrotron; 0.412824	synchrotron; 0.457667	synchrotron; 0.412824
lattice parameters (Å)	a = 11.09060(1)	a = 11.10166(6)	a = 11.10911(7)
	c = 17.41663(6)	c = 17.40089(4)	c = 17.39509(6)
$V(Å^3)$	1855.26(1)	1857.28(5)	1859.15(9)
$R_{ m p}$	0.0874	0.0739	0.0840
$R_{ m wp}$	0.1144	0.0907	0.1090

moisture from the air, resulting in a reaction with BaCO3 and NaHCO₃. Unfortunately, the product is nearly amorphous and could not be indexed to any reported phases due to the phase complexity and low intensity of the diffraction peaks. The subsequent reaction of the aged mixture at 600 °C for 2 h followed by 725 °C for 30 h with an intermediate grinding resulted in a bright green emission upon irradiation with a UV lamp. The green-emitting material can also be prepared without the aging step, although the product includes a mixture of blue- and green-emitting products, suggesting substitution on both the monovalent and divalent sites. Increasing the reaction time or temperature also causes a decrease of the green emission and intensification of the blue emission, supporting the metastable nature of NBBO:Eu_{Na}. A fresh sample of the pure blue-emitting analogue, NBBO:Eu_{Ba}, was also prepared for comparison by immediately reacting the freshly ground powder at 600 °C for 2 h and then at 780 °C for 30 h with an intermediate grinding step. As previously reported, this synthesis route produces a bright blue emission upon irradiation with a UV lamp.

According to the synchrotron powder X-ray diffractograms, 29 shown in Figure 1b and Figure S2, NBBO:Eu_{Na} is nearly phase pure with a minor impurity that belongs to BaB₈O₁₃, whereas NBBO:Eu_{Ba} is a single-phase product. This slight impurity in NBBO:Eu_{Na} is due to the relatively similar synthetic temperature of these phases. Fortunately, Ba-B₈O₁₃:Eu²⁺ emits at ~405 nm, which does not impede the ensuing structural or optical characterization. The morphology of NBBO:Eu_{Na} was examined by using scanning electron microscopy (SEM) and energy-dispersive X-ray spectroscopy (EDS), shown in Figure S3, and shows that Na, Ba, B, O, and Eu are uniformly distributed in the particles examined.

It is challenging to determine the Eu²⁺ site preference because of the similar X-ray scattering power between the rareearth and Ba²⁺. However, the Eu²⁺ substitution can be proven by analyzing the lattice parameters obtained from Rietveld refinements. The refined atom positions and atomic displacement parameters are provided in Tables S1 and S2, and the crystallographic data are provided in Table 1. Comparing the refined unit cell volumes shows that taking the unsubstituted NBBO host and substituting Eu²⁺ with a reaction temperature of 780 °C causes the unit cell volume to decrease. Given that the rare-earth ionic radius is smaller than the alkaline earth, Eu²⁺ is undoubtedly occupying the Ba²⁺ crystallographic position as anticipated for NBBO:EuBa. Conversely, employing the lower reaction temperature (725 °C) shows that the product has a refined lattice parameter larger than the unsubstituted NBBO. This change can only occur if Eu²⁺ substitutes for the smaller Na+ cation causing the unit cell volume to increase. This substitution preference for Eu²⁺ is metastable because continuing the reaction for a longer time or using a temperature >725 °C results in the rare-earth occupying Ba²⁺ site.

Measuring the photoluminescent excitation spectrum of NBBO: Eu_{Na} reveals a broad excitation peak spanning from <280 to \approx 480 nm, as plotted in Figure 2a. This is critical

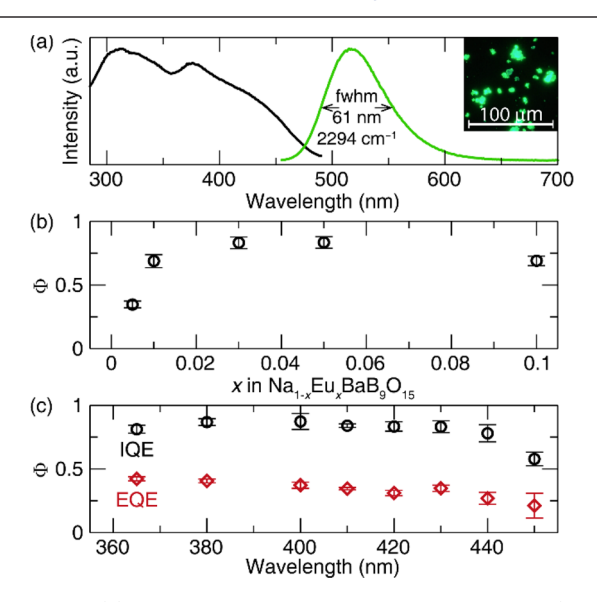


Figure 2. (a) Room-temperature excitation spectrum (black) monitored at 515 nm and emission (green) spectrum excited at 430 nm of NBBO:Eu_{Na}. The inset shows a photograph of the bright green emission produced by this phosphor. (b) Room temperature internal Φ values of Na_{1-x}Eu_xBaB₉O₁₅ substituted with varying concentrations of Eu²⁺ under 430 nm excitation. (c) Room temperature Φ [internal quantum efficiency (IQE) and external quantum efficiency (EQE)] values of NBBO:Eu_{Na} determined by using different excitation wavelengths.

because it indicates the phosphor can be excited by various LED sources making it versatile. The emission spectrum (Figure 2a), when excited with a blue excitation source (λ_{ex} = 430 nm), displays an emission peak with a maximum centered at 515 nm and a full width at half-maximum (fwhm) of ~61 nm (2294 cm⁻¹). The fwhm of the NBBO:Eu_{Na} phosphor is slightly broader than the narrowest commercial green phosphor, β -SiAlON:Eu²⁺ (fwhm = 55 nm; 1760 cm⁻¹), but it is narrower than some well-known green phosphors such as $(Ba_{0.54}Sr_{0.46})_2SiO_4:Eu^{2+}$ (fwhm = 72 nm; 2536 cm⁻¹) and $Y_3(Al,Ga)_5O_{12}:Ce^{3+}$ (fwhm = 120 nm; 3750 cm⁻¹). 12,13,39 The NBBO:Eu_{Na} emission spectra measured by using typical UV and near-UV excitation sources (λ_{ex} = 330, 365, and 395 nm) and blue source (λ_{ex} = 450 nm) all show the same narrow green emission, plotted in Figure S4. It is worth noting that excitation with the deep UV light shows an intense green emission and a small peak in the blue region attributed to a small concentration of Eu²⁺ substituting on Ba²⁺ site. The green emission peak corresponds to the 5d → 4f electronic transition stemming from the Eu2+ occupying the sole

crystallographically independent Na⁺. The single Eu²⁺ site is further supported by measuring the photoluminescence lifetime, as shown in Figure S5. The time-gated photoluminescence data were fit with a single-exponential function to reveal a luminescence lifetime for the green peak in NBBO:Eu_{Na} of 1.103 μ s. This is distinct from the blue emission lifetime in NBBO:Eu_{Ba} of 0.842 μ s. These lifetimes agree with the electronic transitions of Eu²⁺ substituted phosphors and are fast enough to minimize any saturation effects.

It is useful that this phosphor can be excited by blue light and produce a bright green emission, but to be industrially relevant NBBO:Eu_{Na} must also have high efficiency. First, the rare-earth concentration was optimized by varying the loading concentration of Eu²⁺. The X-ray diffractograms indicate the phase purity of the samples, as shown in Figure S6a. The room temperature photoluminescence quantum yield (Φ) , or internal quantum efficiency (IQE), was then measured under 430 nm excitation. As shown in Figure 2b, the 3 mol % Eu²⁺ concentration in NaBaB₉O₁₅:Eu²⁺ has the highest IQE (83%). Increasing the Eu²⁺ concentration to 5% and 10% caused a slight drop in IQE. Because of the broad excitation spectrum, the IQE of the 3% Eu²⁺-doped sample was also measured by using multiple excitation wavelengths to understand its efficiency across the electromagnetic spectrum. As shown in Figure 2c, this phosphor possesses an IQE of ≈80% when excited at 365 nm. The IQE improves as the excitation wavelength shifts to λ_{ex} = 400 nm, which is the highest IQE of 87%. Exciting the phosphor with blue light (λ_{ex} = 430 nm) causes a minor decrease with IQE of 83% while excitation at $\lambda_{\rm ex}$ = 450 nm leads to an IQE of \approx 60%. The external quantum efficiency (EQE) at 3% substitution was also measured and is plotted in Figure 2c. The phosphor has an EQE of 45% upon 365 nm excitation. Using longer wavelength light to excite the phosphor causes a drop in EQE to 24% (λ_{ex} = 450 nm). This EQE is comparable to recently reported green phosphors $RbLi(Li_3SiO_4)_2$: Eu^{2+} and $Ba_{2-x}LiAlS_4$: Eu^{2+} 16,17 The outstanding internal and external quantum efficiency for this phosphor is measured for products directly out of the furnace and could easily be improved with further optimization and postsynthesis processing.

The material's optical properties are greatly affected when integrated into a LED bulb as LEDs operate at ≈ 150 °C (423 K). One of the final tests for any new phosphor before device consideration is measuring the temperature-dependent photoluminescence and the chemical stability of the phosphor.

Evaluating the emission of NBBO:Eu_{Na} from 300 to 700 K under $\lambda_{ex} = 430$ nm (Figure 3a,b) shows an anomalous response where the relative integrated intensity continuously increases compared to the 300 K data before finally entering the quenching regime above 650 K. The relative peak intensity also increases by 10% by 500 K before decreasing. The raw spectra at different temperatures are plotted in Figure S7. The origin of this behavior is attributed to defects in the crystal structure stemming from the aliovalent substitution of Eu²⁺ for Na⁺. According to thermoluminescence measurements (Figure S8), five separate trap states are present in this compound with trap depths of approximately 0.67, 0.73, 0.93, 1.02, and 1.11 eV. Increasing the temperature causes the detrapping of electrons from defects in the compound. This is known to increase the emission intensity as a function of temperature. No detrapping was observed in the original NBBO:Eu_{Ba} report because of the isovalent rare-earth substitution. Nevertheless,

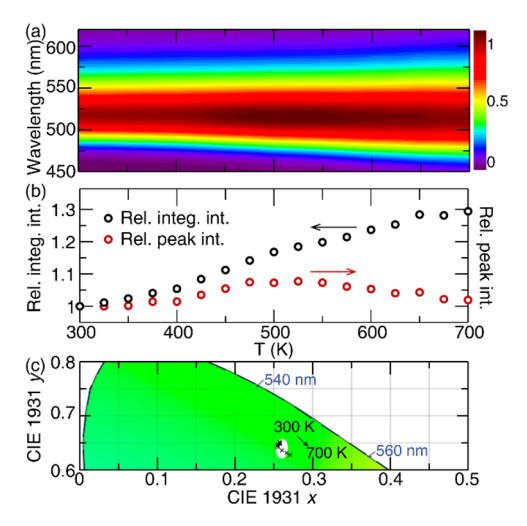


Figure 3. (a) Contour plot of the normalized emission spectra excited at 430 nm as a function of temperature. (b) Relative integrated intensity of the emission spectra (Rel. Integ. Int.) and the relative intensity of the emission peak (Rel. Peak Int.) as a function of temperature. (c) CIE coordinates of the emission color at 300–700 K in 50 K increments. The white ellipse depicts a three-step MacAdam ellipse calculated by using the room temperature emission data.

analyzing the emission color of NBBO:Eu $_{Na}$ as a function of temperature shows all CIE coordinates, except the highest measured temperature (700 K), fall within a three-step MacAdam ellipse, plotted in Figure 3c as the white oval. This signifies that the emission color change is indistinguishable to the average human eye even at extreme temperatures supporting the fact that the phosphor's optical properties robust at nearly all temperatures probed.

A fresh sample of NBBO:E u_{Na} was also annealed in air at 150 °C to determine the oxidation resistance of this phosphor. The powder X-ray diffractograms and optical characteristics were measured on the fresh sample and after 5, 10, and 15 days at this elevated temperature. The results (Figure S9a) show that the phase remains unchanged up to 15 days. The emission spectra collected under 430 nm excitation were also nearly the same except for a tiny blue-shift of the emission spectrum in the sample annealed for 15 days (Figure S9b). The PLQY did drop by 22% after 5 days, although annealing longer caused no further changes (Figure S9c). Finally, the chemical stability against hydrolysis was investigated by dispersing the phosphor in deionized water for 24 h. As shown in Figure S10a, many impurity peaks appeared in the powder X-ray diffractograms after dispersing the sample in water for 15 h. Unfortunately, the new impurity peaks could not be indexed to any known compounds. The existence of impurities does not seemingly influence the normalized emission spectra with the emission peak shape, position, and fwhm remaining nearly identical after 24 h in water (Figure S10b). The PLQY drops by 5%, 40%, and 48% after 6, 15, and 24 h in water, respectively. These results indicate the emission of NBBO:Eu_{Na} has good stability in air, even at high temperatures, and reasonable resistance to moisture.

The bright green color, high efficiency, and thermal robustness of NBBO:EuNa demonstrate this phosphor might be worth considering further for LED-based display applications. A prototype LED device (Device I) focused on potential display applications was therefore fabricated by combining a blue LED chip ($\lambda_{\rm ex} = 450$ nm) with a mixture of

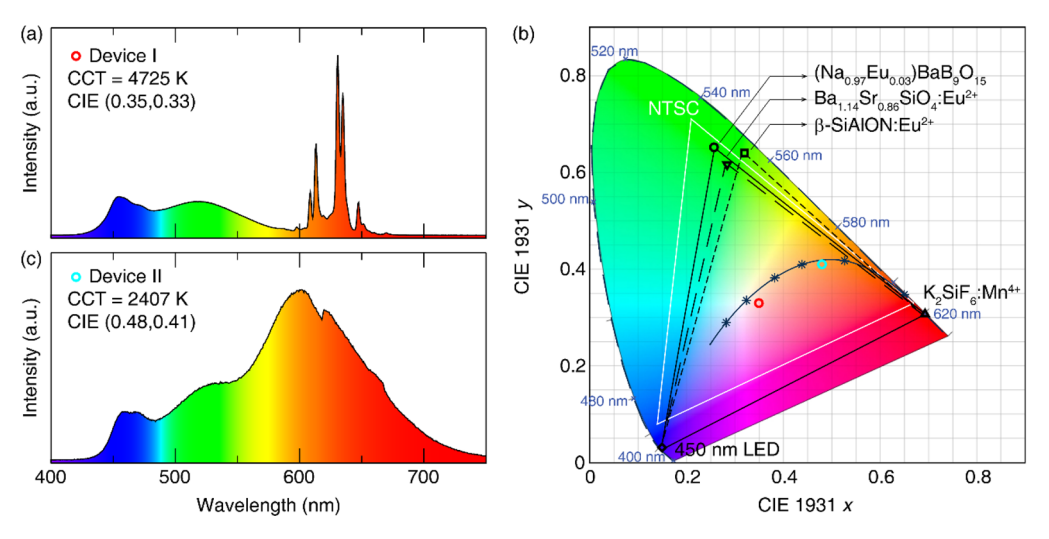


Figure 4. (a) Emission spectrum of the fabricated device I based on 450 nm LED chip, $(Na_{0.97}Eu_{0.03})BaB_9O_{15}$, and $K_2SiF_6:Mn^{4+}$ phosphors. (b) Room temperature CIE coordinates of $(Na_{0.97}Eu_{0.03})BaB_9O_{15}$ (black circle), $Ba_{1.14}Sr_{0.86}SiO_4:Eu^{2+}$ (down-triangle), β-SiAlON: Eu^{2+} (square), $K_2SiF_6:Mn^{4+}$ (up-triangle), and 450 nm LED (diamond). Plotted in gray is the NTSC color space. The CIE coordinates of Devices I and II are shown as the red and blue circles, respectively. (c) Emission spectrum of the fabricated device II is based on a 450 nm LED chip, NBBO: Eu_{Na} , and $Sr_2Si_5N_8:Eu^{2+}$ phosphors.

the as-synthesized green-emitting NBBO: Eu_{Na} and the commercial red-emitting K_2SiF_6 : Mn^{4+} . The device was driven by a current of 20 mA, and the resulting photoluminescence spectrum is shown in Figure 4a. The LED device produces a bright white light (shown as the red circle in Figure 4b) with CIE coordinates of (0.35, 0.33) and a correlated color temperature (CCT) of 4725 K.

The potential in display applications of NBBO: Eu_{Na} is reinforced by plotting the room temperature color coordinates of NBBO:Eu_{Na} alongside the industry-standard green phosphors β-SiAlON:Eu²⁺ and Ba_{1.14}Sr_{0.86}SiO₄:Eu²⁺ on a 1931 CIE diagram (Figure 4b). β-SiAlON:Eu²⁺ emits an almost monochromatic light but with a slight yellow shift. A more significant drawback is that the material requires harsh synthetic conditions (high pressure) to prepare, which increases the phosphor's market price driving up the consumer cost of displays by using β -SiAlON:Eu²⁺. β -SiAlON:Eu²⁺ also falls outside the National Television System Committee (NTSC) color triangle, decreasing the color quality in real display applications. In contrast, NBBO: Eu_{Na} and Ba_{1.14}Sr_{0.86}SiO₄:Eu²⁺ are located within the NTSC triangle with NBBO:Eu_{Na} being closer to the green corner, providing potential improvements to color quality if this material was used in display applications. To ascertain the available color gamut covered if NBBO:EuNa were used in a device, the CIE coordinates were calculated in combination with a blueemitting 450 nm LED and red-emitting K₂SiF₆:Mn⁴⁺. Comparing the area of the resulting triangle created by connecting the coordinates for the LED-NBBO:Eu $_{\mathrm{Na}} K_2SiF_6:Mn^{4+}$ system with the triangle created by LED- β -SiAlON: Eu²⁺ - K₂SiF₆: Mn⁴⁺ and the LED- $Ba_{1,14}Sr_{0,86}SiO_4:Eu^{2+}-K_2SiF_6:Mn^{4+}$ shows that using NBBO:Eu_{Na} broadens the color gamut coverage by 8% compared to these other phosphor systems. In addition, the NBBO:Eu_{Na} based triangle has an area that overlaps with 83% of the NTSC area, which is larger than a device using β -SiAlON:Eu²⁺ (72% of NTSC area) and Ba_{1.14}Sr_{0.86}SiO₄:Eu²⁺ (76% of NTSC area) by permitting more color in the green wavelength region.

This new green phosphor's versatility was further supported by creating a second LED prototype (Device II) for domestic lighting purposes. This warm white light was realized by using a 450 nm LED chip with the as-prepared NBBO:Eu_{Na} and lab-made, red-emitting $\mathrm{Sr_2Si_3N_8:Eu^{2+}}$. The spectrum plotted in Figure 4c exhibits a continuous broadband emission, covering the whole visible region. This gives rise to an excellent overall CRI of 89. Moreover, the CRI of R₁₁ is 90, which is specific to green, is equally high, indicating the spectrum of the resulting device is near ideal for reproducing the green color. The notorious cyan cavity is also covered by the phosphor in the asfabricated device, resulting in outstanding color quality. The overall emission shows a warm white color (depicted as the blue circle in Figure 4b) with CIE coordinates of (0.48, 0.41) and a CCT of 2407 K.

CONCLUSIONS

DFT calculations were conducted to show that Eu²⁺ substitution on the Na⁺ antisite and the isovalent Ba²⁺ site is an energetically competitive process in the NaBaB₉O₁₅ system. A highly efficient green-emitting phosphor, (Na_{0.97}Eu_{0.03})-BaB₉O₁₅ was successfully synthesized by aging the starting materials for 2 weeks and lowering the sintering temperature to drive the substitution of Eu²⁺ onto the smaller, less favorable [NaO₆] substitution site. The resulting phosphor has a high efficiency that makes it competitive with commercial phosphors. Indeed, the phosphor shows a Φ > 80% by using a blue or near-UV LED as the excitation source, and it is thermally robust with a short emission lifetime. The fabricated prototype light bulb using (Na_{0.97}Eu_{0.03})BaB₉O₁₅ and its ease of synthesis suggest this bright green phosphor also supports the outstanding potential in the general white lighting and display lighting space. This phosphor development was achieved by taking advantage of preferential substitution, which has not yet been demonstrated in the phosphor field. These results undoubtedly provide a new approach for researchers to design new phosphors and explore new classes of luminescent materials by controlling rare-earth substitution.

ASSOCIATED CONTENT

Supporting Information

The Supporting Information is available free of charge at https://pubs.acs.org/doi/10.1021/acs.chemmater.1c00447.

Powder X-ray diffractograms, Rietveld refinements, SEM and EDS images, emission spectra excited at different wavelengths, time-gated luminescence decay curve, temperature-dependent emission spectra, thermoluminescence curve, and refined atomic coordinates and isotropic displacement parameters (PDF)

AUTHOR INFORMATION

Corresponding Author

Authors

Ya Zhuo – Department of Chemistry, University of Houston, Houston, Texas 77204, United States; orcid.org/0000-0003-2554-498X

Shruti Hariyani — Department of Chemistry, University of Houston, Houston, Texas 77204, United States; orcid.org/0000-0002-4707-8863

Jiyou Zhong — Department of Chemistry, University of Houston, Houston, Texas 77204, United States;
orcid.org/0000-0003-2817-6617

Complete contact information is available at: https://pubs.acs.org/10.1021/acs.chemmater.1c00447

Notes

The authors declare no competing financial interest.

ACKNOWLEDGMENTS

The authors thank the National Science Foundation (DMR-1847701) as well as the R.A. Welch Foundation (E-1981) for supporting this work. This work used the resources available through the 11-BM beamline at the Advanced Photon Source, an Office of Science User Facility operated for the US Department of Energy (DOE) Office of Science by Argonne National Laboratory, under Contract DE-AC02-06CH11357. This research used the Opuntia/Sabine/Carya cluster(s) operated by the Research Computing Data Core at the University of Houston.

REFERENCES

- (1) Pust, P.; Schmidt, P. J.; Schnick, W. A Revolution in Lighting. *Nat. Mater.* **2015**, *14* (5), 454–458.
- (2) George, N. C.; Denault, K. A.; Seshadri, R. Phosphors for Solid-State White Lighting. *Annu. Rev. Mater. Res.* **2013**, 43 (1), 481–501.
- (3) Liao, H.; Zhao, M.; Molokeev, M. S.; Liu, Q.; Xia, Z. Learning from a Mineral Structure toward an Ultra-Narrow-Band Blue-Emitting Silicate Phosphor RbNa₃(Li₃SiO₄)₄:Eu²⁺. *Angew. Chem.* **2018**, *130* (36), 11902–11905.
- (4) Pust, P.; Weiler, V.; Hecht, C.; Tücks, A.; Wochnik, A. S.; Henß, A.-K.; Wiechert, D.; Scheu, C.; Schmidt, P. J.; Schnick, W. Narrow-Band Red-Emitting Sr[LiAl₃N₄]:Eu²⁺ as a next-Generation LED-Phosphor Material. *Nat. Mater.* **2014**, *13* (9), 891–896.
- (5) Strobel, P.; Maak, C.; Weiler, V.; Schmidt, P. J.; Schnick, W. Ultra-Narrow-Band Blue-Emitting Oxoberyllates AELi₂[Be₄O₆]:Eu²⁺ (AE = Sr,Ba) Paving the Way to Efficient RGB Pc-LEDs. *Angew. Chem., Int. Ed.* **2018**, *57* (28), 8739–8743.

- (6) Kim, Y. H.; Arunkumar, P.; Kim, B. Y.; Unithrattil, S.; Kim, E.; Moon, S.-H.; Hyun, J. Y.; Kim, K. H.; Lee, D.; Lee, J.-S.; Im, W. B. A Zero-Thermal-Quenching Phosphor. *Nat. Mater.* **2017**, *16* (5), 543–550.
- (7) Qiao, J.; Ning, L.; Molokeev, M. S.; Chuang, Y.; Zhang, Q.; Poeppelmeier, K. R.; Xia, Z. Site-Selective Occupancy of Eu²⁺ Toward Blue-Light-Excited Red Emission in a Rb₃YSi₂O₇:Eu Phosphor. *Angew. Chem.* **2019**, *131* (33), 11654–11650.
- (8) Wagatha, P.; Weiler, V.; Schmidt, P. J.; Schnick, W. Tailoring Emission Characteristics: Narrow-Band Red Luminescence from SLA to CaBa[Li₂Al₆N₈]:Eu²⁺. Chem. Mater. **2018**, 30, 7885–7891.
- (9) Duke, A. C.; Hariyani, S.; Brgoch, J. Ba₃Y₂B₆O₁₅:Ce³⁺: A High Symmetry, Narrow-Emitting Blue Phosphor for Wide-Gamut White Lighting. *Chem. Mater.* **2018**, *30*, 2668–2675.
- (10) Zhong, J.; Hariyani, S.; Zhuo, Y.; Zhao, W.; Liu, X.; Wen, J.; Brgoch, J. Combining Experiment and Computation to Elucidate the Optical Properties of Ce³⁺ in Ba₅Si₈O₂₁. *Phys. Chem. Chem. Phys.* **2020**, 22 (4), 2327–2336.
- (11) Hirosaki, N.; Xie, R.-J.; Kimoto, K.; Sekiguchi, T.; Yamamoto, Y.; Suehiro, T.; Mitomo, M. Characterization and Properties of Green-Emitting β -SiAlON:Eu²⁺ Powder Phosphors for White Light-Emitting Diodes. *Appl. Phys. Lett.* **2005**, *86*, 211905.
- (12) Li, S.; Wang, L.; Tang, D.; Cho, Y.; Liu, X.; Zhou, X.; Lu, L.; Zhang, L.; Takeda, T.; Hirosaki, N.; Xie, R.-J. Achieving High Quantum Efficiency Narrow-Band β -SiAlON:Eu²⁺ Phosphors for High-Brightness LCD Backlights by Reducing the Eu³⁺ Luminescence Killer. *Chem. Mater.* **2018**, *30*, 494–505.
- (13) Streit, H.; Kramer, J.; Suta, M.; Wickleder, C. Red, Green, and Blue Photoluminescence of Ba₂SiO₄:M (M = Eu³⁺, Eu²⁺, Sr²⁺) Nanophosphors. *Materials* **2013**, *6* (8), 3079–3093.
- (14) Peters, T. E.; Baglio, J. A. Luminescence and Structural Properties of Thiogallate Phosphors Ce⁺³ and Eu⁺²-Activated Phosphors. Part L. J. Electrochem. Soc. **1972**, 119, 230–236.
- (15) Lei, B.; Sha, L.; Zhang, H.; Liu, Y.; Man, S. Q.; Yue, S. Preparation and Luminescence Properties of Green-Light-Emitting Afterglow Phosphor Ca₈Mg(SiO₄)₄Cl₂:Eu²⁺. *Solid State Sci.* **2010**, *12* (12), 2177–2181.
- (16) Kim, M.; Singh, S. P.; Shim, S.; Park, W. B.; Sohn, K. S. Discovery of a Quaternary Sulfide, Ba_{2-x}LiAlS₄:Eu²⁺, and Its Potential as a Fast-Decaying LED Phosphor. *Chem. Mater.* **2020**, 32 (15), 6697–6705.
- (17) Zhao, M.; Liao, H.; Ning, L.; Zhang, Q.; Liu, Q.; Xia, Z. Next-Generation Narrow-Band Green-Emitting RbLi(Li₃SiO₄)₂:Eu²⁺ Phosphor for Backlight Display Application. *Adv. Mater.* **2018**, *30* (38), 1802489.
- (18) Jang, E.; Jun, S.; Jang, H.; Lim, J.; Kim, B.; Kim, Y. White-Light-Emitting Diodes with Quantum Dot Color Converters for Display Backlights. *Adv. Mater.* **2010**, 22 (28), 3076–3080.
- (19) Song, J.; Li, J.; Li, X.; Xu, L.; Dong, Y.; Zeng, H. Quantum Dot Light-Emitting Diodes Based on Inorganic Perovskite Cesium Lead Halides (CsPbX₃). Adv. Mater. **2015**, 27 (44), 7162–7167.
- (20) Verma, S.; Verma, K.; Kumar, D.; Chaudhary, B.; Som, S.; Sharma, V.; Kumar, V.; Swart, H. C. Recent Advances in Rare Earth Doped Alkali-Alkaline Earth Borates for Solid State Lighting Applications. *Phys. B* **2018**, 535, 106–113.
- (21) Yu, R.; Zhong, S.; Xue, N.; Li, H.; Ma, H. Synthesis, Structure, and Peculiar Green Emission of NaBaBO₃:Ce³⁺ Phosphors. *Dalt. Trans.* **2014**, 43 (28), 10969–10976.
- (22) Zhong, J.; Zhao, W.; Zhuo, Y.; Yan, C.; Wen, J.; Brgoch, J. Understanding the Blue-Emitting Orthoborate Phosphor NaBa-BO₃:Ce³⁺ through Experiment and Computation. *J. Mater. Chem. C* **2019**, 7 (3), 654–662.
- (23) Zhuo, Y.; Mansouri Tehrani, A.; Oliynyk, A. O.; Duke, A. C.; Brgoch, J. Identifying an Efficient, Thermally Robust Inorganic Phosphor Host via Machine Learning. *Nat. Commun.* **2018**, 9 (1), 4377.
- (24) Penin, N.; Seguin, L.; Touboul, M.; Nowogrocki, G. Synthesis and Crystal Structure of Three $MM'B_9O_{15}$ Borates (M = Ba, Sr and

- M'=Li; M = Ba and M'=Na). Int. J. Inorg. Mater. 2001, 3 (7), 1015–1023.
- (25) Hafner, J. Ab-Initio Simulations of Materials Using VASP: Density-Functional Theory and Beyond. *J. Comput. Chem.* **2008**, 29 (13), 2044–2078.
- (26) Blöchl, P. E. Projector Augmented-Wave Method. Phys. Rev. B: Condens. Matter Mater. Phys. 1994, 50 (24), 17953–17979.
- (27) Perdew, J. P.; Burke, K.; Ernzerhof, M. Generalized Gradient Approximation Made Simple. *Phys. Rev. Lett.* **1996**, 77 (18), 3865–3868.
- (28) Brito, H. F.; Felinto, M. C. F. C.; Hölsä, J.; Laamanen, T.; Lastusaari, M.; Malkamäki, M.; Novák, P.; Rodrigues, L. C. V.; Stefani, R. DFT and Synchrotron Radiation Study of Eu²⁺ Doped BaAl₂O₄. Opt. Mater. Express **2012**, 2 (4), 420.
- (29) Lee, P. L.; Shu, D.; Ramanathan, M.; Preissner, C.; Wang, J.; Beno, M. A.; Von Dreele, R. B.; Ribaud, L.; Kurtz, C.; Antao, S. M.; Jiao, X.; Toby, B. H. A Twelve-Analyzer Detector System for High-Resolution Powder Diffraction. *J. Synchrotron Radiat.* **2008**, *15* (5), 427–432.
- (30) Larson, A. C.; Von Dreele, R. B. General Structure Analysis System (GSAS) (Report LAUR); Los Alamos, New Mexico, 2004.
- (31) Toby, B. H. EXPGUI, A Graphical User Interface for GSAS. J. Appl. Crystallogr. 2001, 34 (2), 210–213.
- (32) Leyre, S.; Coutino-Gonzalez, E.; Joos, J. J.; Ryckaert, J.; Meuret, Y.; Poelman, D.; Smet, P. F.; Durinck, G.; Hofkens, J.; Deconinck, G.; Hanselaer, P. Absolute Determination of Photoluminescence Quantum Efficiency Using an Integrating Sphere Setup. *Rev. Sci. Instrum.* 2014, 85 (12), 123115.
- (33) Shannon, R. D. Revised Effective Ionic Radii and Systematic Studies of Interatomie Distances in Halides and Chaleogenides. *Acta Crystallogr., Sect. A: Cryst. Phys., Diffr., Theor. Gen. Crystallogr.* **1976**, A32, 751–767.
- (34) Wang, Y.; Xu, X.; Yin, L.; Hao, L. High Thermal Stability and Photoluminescence of Si–N-Codoped BaMgAl₁₀O₁₇:Eu²⁺ Phosphors. *J. Am. Ceram. Soc.* **2010**, *93* (6), 1534–1536.
- (35) Lu, F.-C.; Bai, L.-J.; Yang, B.-Z.; Yang, Z.-P. Synthesis, Structure and Photoluminescence of BaAl₂Si₂O₈:Eu²⁺ Blue-Emitting Phosphors. *ECS J. Solid State Sci. Technol.* **2013**, 2 (11), R254–R257.
- (36) Hume-Rothery, W.; Powell, H. M. On the Theory of Super-Lattice Structures in Alloys. *Z. Kristallogr. Cryst. Mater.* **1935**, 91 (1-6), 23–47.
- (37) Van Uitert, L. G. An Empirical Relation Fitting the Position in Energy of the Lower D-Band Edge for Eu²⁺ or Ce³⁺ in Various Compounds. *J. Lumin.* **1984**, 29 (5-6), 1–9.
- (38) He, L.; Wang, Y.; Sun, W. Luminescence Properties of BaB_8O_{13} :Eu under UV and VUV Excitation. *J. Rare Earths* **2009**, 27 (3), 385–389.
- (39) Wako, A. H.; Dejene, F. B.; Swart, H. C. Effect of Ga³⁺ and Gd³⁺ Ions Substitution on the Structural and Optical Properties of Ce³⁺ -Doped Yttrium Aluminium Garnet Phosphor Nanopowders. *Luminescence* **2016**, *31* (7), 1313–1320.
- (40) MacAdam, D. L. Visual Sensitivities to Color Differences in Daylight. J. Opt. Soc. Am. 1942, 32, 247-274.
- (41) Zhong, J.; Zhuo, Y.; Hariyani, S.; Zhao, W.; Wen, J.; Brgoch, J. Closing the Cyan Gap Toward Full-Spectrum LED Lighting with NaMgBO₃:Ce³⁺. Chem. Mater. **2020**, 32 (2), 882–888.
- (42) Zhao, M.; Liao, H.; Molokeev, M. S.; Zhou, Y.; Zhang, Q.; Liu, Q.; Xia, Z. Emerging Ultra-Narrow-Band Cyan-Emitting Phosphor for White LEDs with Enhanced Color Rendition. *Light: Sci. Appl.* **2019**, 8 (1), 38
- (43) Strobel, P.; De Boer, T.; Weiler, V.; Schmidt, P. J.; Moewes, A.; Schnick, W. Luminescence of an Oxonitridoberyllate: A Study of Narrow-Band Cyan-Emitting Sr[Be₆ON₄]:Eu²⁺. *Chem. Mater.* **2018**, 30, 3122–3130.
- (44) You, S.; Zhuo, Y.; Chen, Q.; Brgoch, J.; Xie, R. J. Dual-Site Occupancy Induced Broadband Cyan Emission in Ba₂CaB₂Si₄O₁₄:Ce³⁺. *J. Mater. Chem. C* **2020**, 8 (44), 15626–15633. (45) Fang, M.-H.; Ni, C.; Zhang, X.; Tsai, Y.-T.; Mahlik, S.;

Lazarowska, A.; Grinberg, M.; Sheu, H.-S.; Lee, J.-F.; Cheng, B.-M.;

Liu, R.-S. Enhance Color Rendering Index via Full Spectrum Employing the Important Key of Cyan Phosphor. *ACS Appl. Mater. Interfaces* **2016**, *8*, 30677–30682.